

Electronic Supplementary Information

**Monolithic Scaffolds for Highly Selective Ion Sensing/Removal of
Co(II), Cu(II), and Cd(II) Ions in Water**

M.A. Shenashen,^a Sherif A. El-Safty,^{a,b,*} E.A. Elshehy,^a

^a National Institute for Materials Science (NIMS), 1-2-1 Sengen, Tsukuba-shi, Ibaraki-ken, 305-0047,
Japan.

^b Graduate School for Advanced Science and Engineering, Waseda University, 3-4-1 Okubo, Shinjuku-ku,
Tokyo, 169-8555, Japan.

Tel: +81-298592135 Fax: +81-298592025

E-mail: sherif.elsafty@nims.go.jp; sherif@aoni.waseda.jp

Experimental:

Synthesis and characterization of dicarboxylate 1-(phenylamino)-3-phenylimino-thiourea (DCPPT)

Chromophore molecule dicarboxylate 1-(phenylamino)-3-phenylimino-thiourea (DCPPT) was synthesized by dissolving 2 M 4-hydrazinobenzoic acid (3 g, Aldrich) in 30 mL 0.15% NaOH. Approximately 20 mL ethanol and 0.77 g (0.1 M) CS₂ were then added. The mixture was refluxed for 6 h, and ethanol (100 mL) was added upon cooling. The resulting product was obtained in acidic solution with the addition of 0.1 M hydrochloric acid and had a pH of 5. The probe was thoroughly washed with deionized water, centrifuged, filtered, and then dried.

Synthesis of cubic Im3m, Ia3d and Pm3n aluminosilica monoliths

A family of highly ordered cubic cage aluminosilica monoliths was synthesized by using triblock copolymers (P123, F68, and F108) in the instantly direct templating liquid-crystal phase, as recently reported.^{37,38} For example, synthesis of cubic *Im3m* cage-like monoliths at a F108/(Si/Al) mass ratio of 35 wt % in the lyotropic systems was as follows.

Mesocage body-centred-cubic *Im3m* aluminosilica monoliths (with Si/Al ratios of 9) fabricated by using microemulsion phases of F108 surfactant were used as scaffolds. Under typical synthesis conditions of the mesocage *Im3m* scaffold, the precursor solution (0.72 g of F108 surfactant, 0.18 g C₁₂-alkane, 1.8 g of TMOS, and 0.256 g of Al(NO₃)₃·9H₂O) was mixed and then shaken at 50 °C until it became homogeneous, then 2.25 g of H₂O–HCl (pH = 1.3) was quickly added to this solution. The flask that contained the synthesis composition was instantly connected to the rotary evaporator (EYELA NVC-2100) at 45 °C and at a starting pressure of 1023 hPa. After evacuation for 15 min, the resulting optical gel-like aluminosilica materials acquired the shape and size of the reaction vessel. The resultant surfactant/aluminosilica solid was gently dried at room temperature for 3 h and then allowed to stand in a sealed container at 25 °C for 1 day to complete the drying process.

Monoliths with gyroidal cubic *Ia3d* aluminosilica monoliths (with Si/Al ratios of 9) fabricated by using microemulsion phases of F68 surfactant were used as scaffolds. Under typical synthesis conditions of the mesocage *Ia3d* scaffold as mentioned above, the precursor solution (1.023 g of F68 surfactant, 1.8 g of TMOS, and 0.256 g of Al(NO₃)₃·9H₂O) was mixed and then shaken at 50 °C until it became homogeneous, then 2.25 g of H₂O–HCl (pH = 1.3) was quickly added to this solution.

Monoliths with primitive cubic *Pm3n* cage structures were fabricated based on phase transition induced by the addition of 0.51 g of TMB to the cubic *Ia3d* phase domains of F68. The amount ratio of copolymers to aliphatic hydrocarbons (alkane) was kept at 2:0.5, however, this amount ratio was increased to 2:1 when TMB was used as a solublizing agent added to the microemulsion phase designs to optimize both the swelling and the interfacial surface curvature of the copolymer micelles. The copolymer and the incorporated TMB and alkanes were removed by calcination. The organic moieties were then removed by calcination at 550 °C for 7 h.

Results and Discussion:

The fine-tuning surfaces of aluminosilica carriers and the combinatorial immobilization of organic moieties with a high loading capacity of numerous DCPPT chelates were achieved via extremely robust sequences during the fabrication of ASOS. This result was proven by the TG-DTA analyses, FTIR spectroscopies, ²⁷Al NMR, NH₃–TPD, and zeta-potential studies (Figs. S1 and S2).

The coordination among aluminum species was investigated using ^{27}Al NMR, as shown in Table S1. In all aluminosilica monoliths and captors, two ^{27}Al peaks were centered at the chemical shift of -1 and 58 ppm, indicating the existence of octahedral (Al^{VI} , AlO_6 , extra framework) and tetrahedral (Al^{IV} , AlO_4 , framework) aluminum sites, respectively. The tetrahedrally coordinated aluminum sites significantly increased with increasing aluminum content in the mesoporous monoliths. The surface acidity of the aluminosilica monoliths was evidenced by the two resultant NH_3 desorption peaks at approximately 200 $^\circ\text{C}$ and by a small, broad peak at approximately 250 $^\circ\text{C}$ to 550 $^\circ\text{C}$ (Table S1). The results clearly indicated that ammonia is desorbed from the weak Lewis and mildly strong *Brønsted* acid sites of the OH^- groups of the aluminosilica carriers (Liu, 2010). In general, these natural surfaces of acid sites strongly induce H-bonding and dispersive interactions with the ligand receptors, leading to the formation of stable sensors/captors without receptor leaching during the sensing assays of the metal ions (Liu, 2010; White, 2007; Yari 2006).

Table S1. ^{27}Al NMR Analyzing data for cubic aluminosilica monolithic captors. ^{27}Al MAS NMR and NH_3 -TPD analyses of the cubic Im3m aluminosilica monoliths and ion-optical sensor.

Sample	^{27}Al Mass NMR			NH_3 -TPD	
	Coordination type	δ ppm	% peak	Desorption centered peak at T/ $^\circ\text{C}$	% amount
Cubic Im3m Monolith Scaffolds	Al^{VI} , AlO_6	-1	49.12	180	70.3
	Al^{IV} , AlO_4	58	50.18	450	29.7
Cubic Im3m Cd(II) ion-Captor	Al^{VI} , AlO_6	-1	54.25	200	75.3
	Al^{IV} , AlO_4	57	45.75	460	24.7

Different aluminosilica materials were characterized using FTIR spectra. As shown in Fig. S1, the systematic design of Aluminosilica optical sensor (ASOS) was based on a densely patterned chromogenic receptor (DCPPT). As a selective binding site for aluminosilica, cubic Im3m aluminosilica and Cd(II) ions were used as examples of aluminosilica materials and uptake process, respectively. With aluminosilica monoliths, DCPPT-modified carriers, and uptake samples, the appearance of a broad absorption band in the 3000 cm^{-1} to 3500 cm^{-1} region indicated the presence of Si-OH asymmetric stretching. In addition, three defined bands at 1250 , 1100 , and 960 cm^{-1} were assigned to Si-O-Al, Si-O-Si, and Si-OH stretching vibrations, respectively (Xu, 2007). The ASOS showed additional absorption bands at 2960 and 1400 cm^{-1} , which were due to the aliphatic C-H and the stronger C-N bonds, respectively (Weng, 2007). No significant changes in these absorption bands were observed after the addition of the DCPPT chelate, indicating the stability of the Cd(II) ion-optical captor systems. The loading capacity of the immobilized DCPPT chelate moieties onto the surface carriers was revealed based on thermal and spectroscopic techniques. The TG curves revealed that DCPPT chelate moieties (Fig. S2) decreased in mass at approximately 180 $^\circ\text{C}$ to 660 $^\circ\text{C}$. This decrease accompanied exothermic peaks in the corresponding DTA

curves, indicating the decomposition of the organic components. The decrease in DCPPT chelate moieties, for example, was 13.76 mass%, which coincided with the adsorption capacity (X, 0.007 mmol/L) of the loaded organic moieties of these materials.

Scheme 1 shows the 3D structure of the DCPPT probe and its corresponding Co(II), Cu(II) and Cd(II) complexes. The symmetrical charge distributions in the two phenolic rings allow plane-structure stability. This flat structure is capable of forming highly ordered complexes. The unique orbital contribution reveals high DCPPT activity through both central and terminal functional group binding sites. The electronegativity associated with the SH group enabled the formation of bonds with divalent metal ions. Furthermore, deprotonation/protonation of NH groups played a key role in the formation of M-to-DCPPT complexes. The pH value was the key factor in the stability of visible color intensity of the [M-DCPPT]_n⁺ complexes formed to generate configurations that were square planar for [Cd-(DCPPT)₂] (E=-721.58 A.U.), tetrahedral for [Co-DCPPT]²⁺ (E=-748.99 A.U.) and [Cu-DCPPT]²⁺ (E=-878.67A.U.) over a wide range of pH values (1–13). A square planar coordination of metal complexes with the Cd(II) ions, at the relatively high pH of 9.5, was achieved due to the link between the sulfur and nitrogen atoms. Stabilization energy is considered a key parameter of selectivity because complex formation is mostly pH dependent. However, Tetrahedral configurations were formed by the metal ions coordinated with the unprotonated form of DCPPT (pH > 5) in which sulfur and nitrogen atoms occupied the corners of the tetrahedral configuration around the central ions. (Scheme 1F-H). The visible color changes were the result of the pH-dependent coordination of the DCPPT donor species with the metal ions and the subsequent stabilization of the complexes. Moreover, the DCPPT donor species in stabilized metal complexes formed a five-membered ring due to a deficiency in the d-orbits of the metal ion centers has been showed. Furthermore, the stability of the highly ordered complexes resulted from the symmetrical distribution of DCPPT around the metal ions.

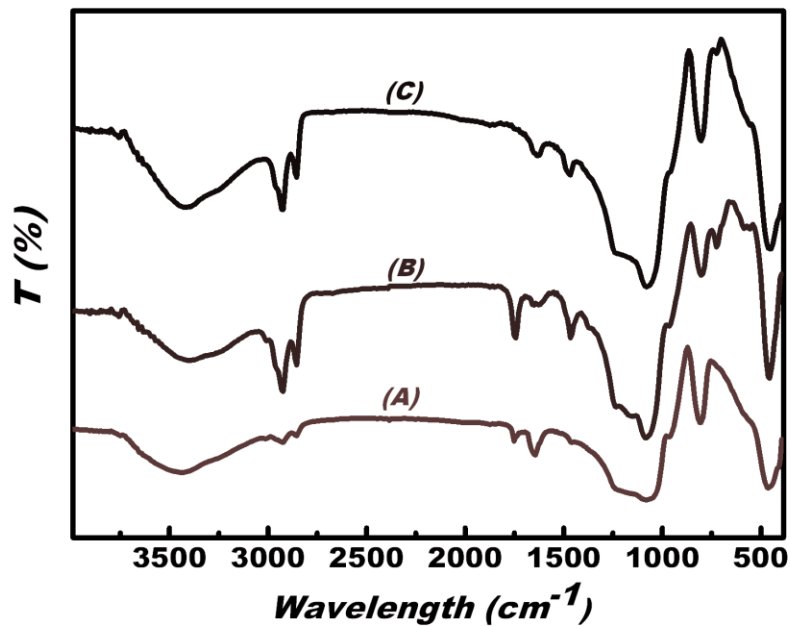


Fig. S1 FTIR characteristics of the 3D Im3m aluminosilica monoliths (A), Aluminosilica optical sensor (ASOS) (B), and aluminosilica optical sensor (ASOS)after Cd(II) ions adsorption (C).

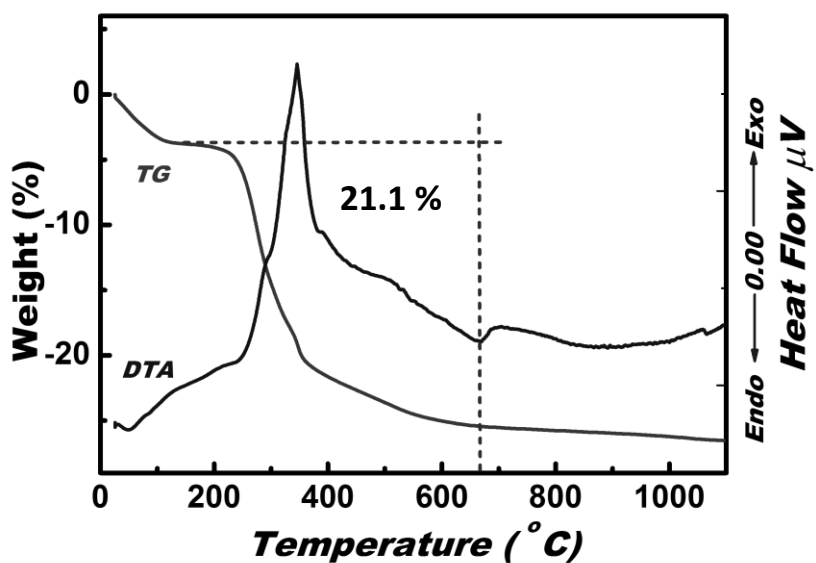


Fig. S2 TGA and DTA analyses of aluminosilica optical sensor (ASOS).

Effect of ASOS pore geometry on the ion-sensing functionality

Figure S3 showed that the ion transport and the affinity of the metal–ligand binding were significantly affected by the structural mesopore geometry and shape of the fabricated cubic ASOS, as clearly shown by the change in the t_R value. Among all ion-sensing systems the cubic cage sensor with bicontinuous pore connection and centrosymmetric phase of cubic $Ia3d$ symmetry exhibited easy accessibility of metal ions and fast M-ligand-binding events. Results indicated that changes in these hierarchical mesocage shapes into the cubic structural symmetry of the sensors can play significant roles in the redistribution of the electron and energy transfer within the binding events of the probe molecule with metal ions into the pore surfaces. Therefore, the chemical sensing system is sensitive to such pore shape changes, which, in turn, acutely affects the kinetic assessment during the determination and visual detection processes of the target ions. Furthermore, the ASOS design was uniquely characterized by a capacious hollow cage shell structure that can encapsulate different types of functional groups and protect the immobilized probe (DCPPT) to maintain the strength of the electron acceptor and donor. The functionalized, shaped, and connecting pores with mesoporous cubic $Pm3n$, $Ia3d$, and $Im3m$ phase domains render the selective adsorption of target ions into interfaced cavities to be vital for the development of the loading capacity, wrapping, and for an efficient ASOS. The structural ordering features of mesoporous aluminosilica architectures allowed ASOS structure to retain an orderly mesostructure that does not distort over the wide pH range (i.e., 1 to 13) required for the sensing and capturing assays. Therefore, this material can be used for the adsorption of distinct target ions as well as pore diffusivity.

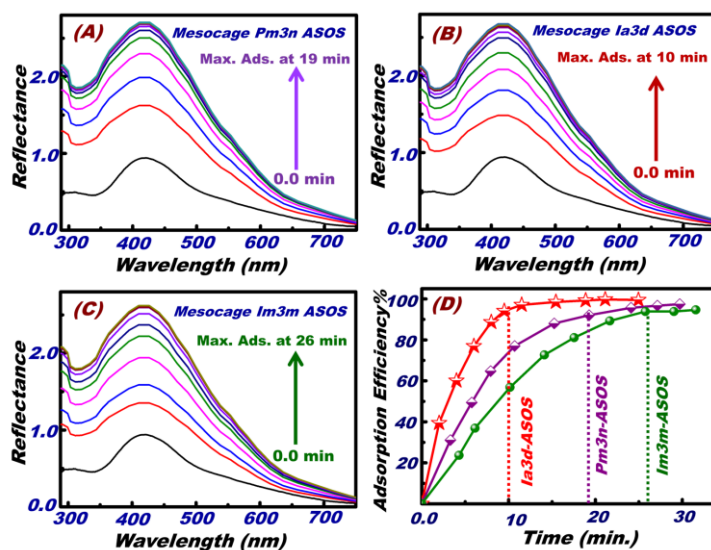


Fig. S3 Hierarchally mesostructured effect of cubic pore geometry and mesocage shape and size of (A) $Pm3n$, (B) $Ia3d$, and (C) $Im3m$ on the [2 ppm] Co(II) ion-sensing functionality of ASOS, as shown from the kinetic time-dependence studies of reflectance spectra response during the formation of $[Co(II)-DCPPT]^{n+}$ complex as function of time and at sensing condition of pH 7, volume 20 ml, 20 mg and at 25 °C. (D) The adsorption efficiency (%) of addition [2ppm] Co(II) ion as function of time using cubic $Pm3n$ -, $Ia3d$ - and $Im3m$ -ASOS at λ_{max} at 409 and pH 7. The finding indicated the effect of cubic crystal lattice and pore organization and atomic structural arrangement on the fast response time of the maximum signaling formation of $[Co(II)-DCPPT]^{n+}$ complex.

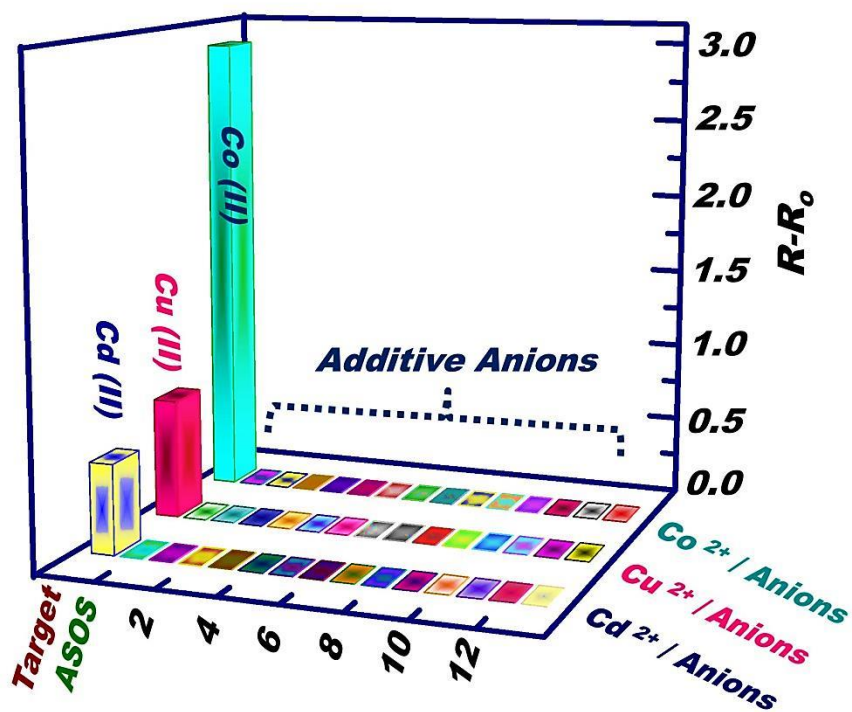


Fig. S4 Representative selectivity profiles of Co(II), Cu(II), and Cd(II) ion-nanocaptors in the presence of various anions of [2 ppm] Target ions at optimal pH values and other capture conditions (amount of 20 mg, volume of 20 mL, and temperature of 25 °C). The interfered anions are the following [listed in order (1 to 13)]: CTAB, Triton X, SDS, citrate, oxalate, tartrate, phthalate, acetate, nitrite, nitrate, sulfite, sulfate, and phosphate.

Adsorption performance of the metal ion capturing system

The batch adsorption processes of target metal ions were performed in normal (matrix free) or in naturally occurring environmental fluids at ion-selective conditions. ICP-MS analysis was used to identify and determine the concentrations of the various constituents. ICP data indicated that the natural samples contained approximately 15.7 mg/dm³ to 265 mg/dm³ of alkali and alkaline earth metal ions, aside from traces of Mn²⁺, Sb³⁺, and Sn²⁺ ions (0.02 mg/dm³ to 0.083 mg/dm³). In these samples, various concentrations of target ions (from 0.001 mg/dm³ to 2.0 mg/dm³) were spiked. The efficient adsorption behavior of the ASOS meso-sensor/captor was verified in terms of loading capacity and efficient binding at the ultra-trace level of target ion concentrations. Adsorption isotherms provided information on how an adsorption system proceeds and measured the interaction efficiency of a specific adsorbent with target ions. The Langmuir isotherm often describes monolayer adsorption. This model assumes a uniform energy of adsorption and a single layer of adsorbed solute at constant temperature. The monolayer coverage and removal characteristics of metal ions on the ASOS surface at constant temperature is represented by the Langmuir isotherm (Fig. 8), which is written as follows:⁵⁷

$$C_e/q_e = 1/(K_L q_m) + (1/q_m)C_e$$

where q_m (mg/g) is the amount of metal ions removed to form a monolayer coverage and K_L is the Langmuir adsorption equilibrium constant. The monolayer coverage can be obtained from a plot of C_e/q_e versus C_e (Fig. S5), which exhibits a straight line. The linear adsorption curves indicate two key components: (1) a wide range of target ion concentrations can be removed in a one-step treatment and (2) the monolayer coverage of the target ions in the interior pore surfaces of mesoporous ASOS captors can be formed with these removal system assays. The practical adsorption capacity q_m and the Langmuir coverage constant K_L were respectively obtained from the slope and intercept of the linear plot. The linear removal curves indicated that a wide range of metal ion concentrations can be removed from aqueous water with high adsorption efficiency of approximately 94% to 96%. These results indicated that the practical removal of 1 g of Co(II), Cu(II), and Cd(II) ions from an aqueous solution requires approximately 4.674, 5.156, and 4.57 g of ASOS captor, respectively.

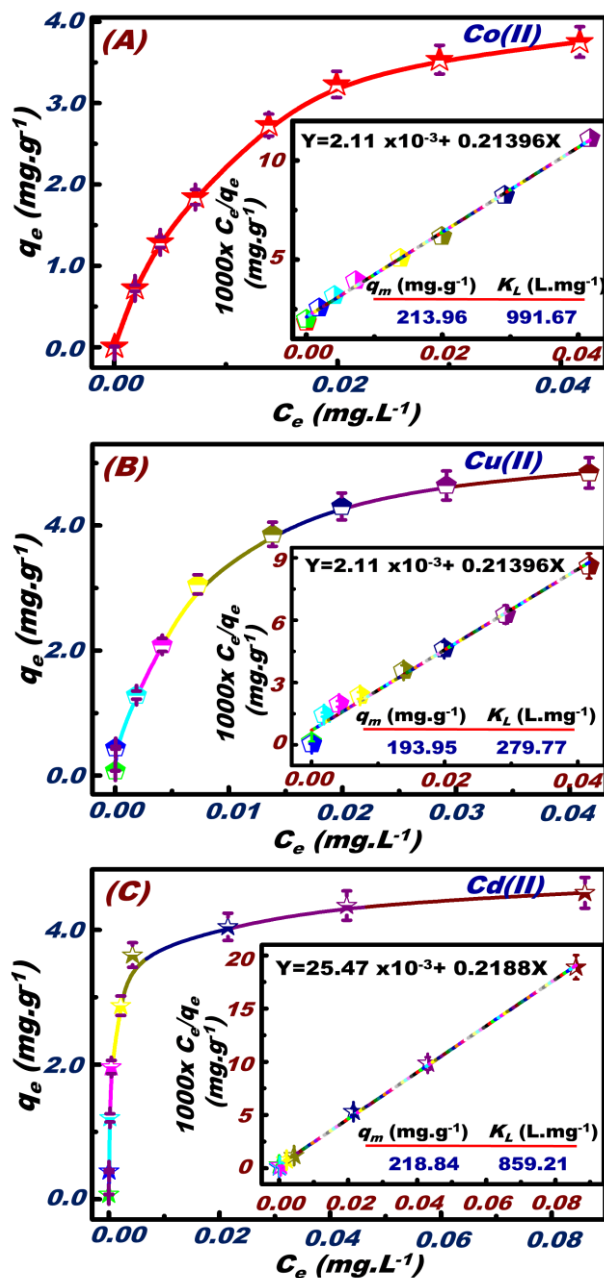


Fig. S5 The adsorption isotherms and the linear form of the Langmuir isotherms (inserts) of Co(II), Cu(II), and Cd(II) target ions onto cage alminosilica-based adsorbents (10 g/L) at pH 7, 9.5, and 12.5, respectively, with a response time of 20 min and temperature of 25 °C.